Role of Mitochondria in Calcium Regulation of Spontaneously Contracting Cardiac Muscle Cells

David N. Bowser,* Tetsuhiro Minamikawa,*# Phillip Nagley,# and David A. Williams*

*Confocal and Fluorescence Imaging Group, Department of Physiology,The University of Melbourne, Parkville, Victoria 3052, and the #Department of Biochemistry and Molecular Biology, Monash University, Clayton, Victoria 3168, Australia

ABSTRACT Mitochondrial involvement in the regulation of cytosolic calcium concentration ($[Ca^{2+}]_i$) in cardiac myocytes has been largely discounted by many authors. However, recent evidence, including the results of this study, has forced a reappraisal of this role. $[Ca^{2+}]_i$ and Ca^{2+} in the mitochondria ($[Ca^{2+}]_m$) were measured in this study with specific fluorescent probes, fluo-3 and di-hydro-rhod-2, respectively; mitochondrial membrane potential ($\Delta\Psi_m$) was monitored with JC-1. Addition of uncouplers or inhibitors of the mitochondrial respiratory chain was found to cause a twofold decrease in the rate of removal of Ca^{2+} from the cytosol after a spontaneously generated Ca^{2+} wave. These agents also caused a progressive elevation of $[Ca^{2+}]_i$, an increase in the number of hotspots of Ca^{2+} release (Ca^{2+} sparks), and depression of mitochondrial potential. The Ca^{2+}-indicative fluorophore dihydro-rhod-2 has a net positive charge that contributes to selective accumulation by mitochondria, as supported by its co-localization with other mitochondrial-specific probes (MitoTracker Green). Treatment of dihydro-rhod-2-loaded cells with NaCN resulted in rapid formation of "black holes" in the otherwise uniformly banded pattern. These are likely to represent individual or small groups of mitochondria that have depressed mitochondrial potential, or have lost accumulated rhod-2 and/or Ca^{2+}; all of these eventualities are possible upon onset of the mitochondrial permeability transition. Release of Ca^{2+} from the sarcoplasmic reticulum and the resultant spontaneous contractility of cardiac muscle are proposed to be triggered by the induction of the mitochondrial permeability transition and the subsequent loss of $[Ca^{2+}]_m$.

INTRODUCTION

The regulation of intracellular free calcium concentration ($[Ca^{2+}]_i$) is important in the life and death of cells. Calcium has a central role in the control of cell function, including the regulation of contractile activity (reviewed by Fay et al., 1988). Important components in this regulation occur through the calcium-sequestering and storage capacity of the sarcoplasmic reticulum (SR) and sarcolemmal influx pathways, which represent the predominant sources of calcium for activation of contraction. The buffering capacity of the cell constituents, notably calcium-binding sites on regulatory proteins such as troponin-C, as well as extrusion activity of the cell membrane (Na^+/Ca^{2+} exchanger and Ca^{2+}-ATPase pumps), provide limits for the elevations of calcium that occur during normal cardiac contractile function (Bers, 1991).

Many laboratories have investigated the properties of propagated spontaneous calcium release (now commonly known as calcium waves) and spontaneous contractility in apparently calcium-overloaded cardiac myocytes (Takamatsu and Wier, 1990; Ishide et al., 1990; Williams, 1993; Lopez et al., 1995). In our own studies (Williams, 1990; Williams et al., 1992), calcium-overloaded cells were seen frequently to generate spontaneous contraction seen as localized bands of contraction and fueled by propagating calcium waves. A direct link between spontaneous contractility due to calcium wave propagation, and the subsequent depolarization, global elevation of intracellular calcium, and cell contraction was clear. This sequence of events would form the basis of an arrythmogenic response.

A major contribution from mitochondria in cellular calcium homeostasis has been largely dismissed, except in conditions of extreme calcium overload experienced by cardiac muscle cells under pathological circumstances. However, this has now been challenged in several studies that have shown a role for mitochondrial involvement in cellular calcium homeostasis under normal physiological conditions (Ichas et al., 1994; Mix et al., 1994; Jouaville et al., 1995; Drummond and Fay, 1996; Ichas et al., 1997; Trollinger et al., 1997). One such study demonstrated that mitochondrial calcium uptake is a major factor in the regulation of inositol-1,4,5-trisphosphate-induced calcium release in *Xenopus* oocytes (Jouaville et al., 1995). A subsequent study in smooth muscle cells found mitochondria to contribute to removal of cytosolic calcium after electrical stimulation (Drummond and Fay, 1996).

Mitochondrial Ca^{2+} ($[Ca^{2+}]_m$) is regulated through transport mechanisms on the inner membrane (reviewed by Gunter and Pfeiffer, 1990; McCormack et al., 1990). They consist of mechanisms for both Ca^{2+} uptake and efflux. Uptake of Ca^{2+} is through the potential-dependent Ca^{2+} uniporter, a mechanism driven by the mitochondrial membrane potential ($\Delta\Psi_m$) through the extrusion of protons by

Received for publication 12 December 1997 and in final form 25 June 1998.

In memory of my postdoctoral mentor Fredric (Fred) S. Fay: your guidance, inspiration, and friendship are with me always (D.A. Williams).

Address reprint requests to Dr. David N. Bowser, Department of Physiology, University of Melbourne, Confocal and Fluorescence Imaging Group, Parkville, VIC 3052, Australia. Tel.: 61-3-9344-5816; Fax: 61-3-9344-5818; E-mail: d.bowser@physiology.unimelb.edu.au.

0006-3495/98/10/2004/11 $2.00

the electron transport chain. Two possible pumping mechanisms have been identified for the efflux of Ca^{2+}: a $2Na^+/Ca^{2+}$ exchanger, linked to electron transport chain proton pumping via Na^+/H^+ exchange, and a Na^+-independent mechanism, known to be a nonelectrogenic $Ca^{2+}/2H^+$ exchanger (Puskin et al., 1976).

The demonstration that accumulation of mitochondrial calcium resulted in the selective permeabilization of the mitochondrial membrane, particularly to Ca^{2+}, provided evidence for an additional pathway for Ca^{2+} efflux (Hunter and Haworth, 1979a,b; Haworth and Hunter, 1979). This process, now known as the mitochondrial permeability transition (MPT), may be due to a large proteinaceous pore, which is thought to span the inner and outer mitochondrial membranes and allows for passage of substrates less than 1.5 kDa (reviewed by Zoratti and Szabo, 1995; Mignotte and Vayssiere, 1998). In addition to a central role in cell death pathways (Marchetti et al., 1996), the MPT has been implicated in the mitochondrial Ca^{2+} overload that ensues from pathophysiological states such as cardiac ischaemia-reperfusion injury (Crompton and Costi, 1990; Griffiths and Halestrap, 1995).

The aim of this study was to investigate whether mitochondrial function has a critical influence on the Ca^{2+} wave characteristics, including initiation frequencies, propagation rates, peak levels, and time course of Ca^{2+} changes. A specific goal was to determine whether the MPT might directly alter Ca^{2+} waves as a consequence of pore opening. As the MPT is sensitive to changes in $\Delta\Psi_m$, we have used a variety of mitochondrial respiratory inhibitors or uncouplers of oxidative phosphorylation to depress $\Delta\Psi_m$. As a decline in $\Delta\Psi_m$ will result in a reduction in mitochondrial calcium uptake, it was also essential to investigate the role the mitochondrial Ca^{2+} uniporter may play in spontaneous calcium waves.

MATERIALS AND METHODS

Isolation of rat left ventricular myocytes

Single ventricular myocytes were isolated from Sprague-Dawley rats as described previously (Williams et al., 1992). Once isolated, the cells were resuspended in *N*-2-hydroxyethlpiperazine-*N*′-2-ethanesulfonic acid (HEPES)-buffered medium containing trypsin inhibitor. Cells were allowed to settle on to a 22 × 40 mm glass coverslip in a solution containing (in mM): 118 NaCl, 4.8 KCl, 1.2 $MgSO_4$, 1.2 KH_2PO_4, 25.0 Na-HEPES, 11.0 glucose, and 1.0 $CaCl_2$. All experiments were conducted at room temperature (20–23°C) within 5 h of cell isolation. Spontaneously contracting myocytes were used in these experiments except where indicated.

Confocal microscopy

Single myocytes loaded with particular fluorescent probes were imaged with a BioRad MRC-1000 laser-scanning confocal microscope coupled to a Nikon Diaphot 300 microscope. The objective lens was a Nikon 60× N.A. 1.4 planapochromat, oil immersion lens. Probes were excited with the 488-nm or 514-nm lines of a 100-mW argon ion laser. Intensity of excitation light was minimized through use of 1% (fluo-3) or 3% (JC-1, Rhod-2, and MitoTracker Green) neutral density filters to curb photobleaching.

Investigations of cytosolic calcium fluxes were made with fluo-3/AM (acetoxymethyl ester). Fluo-3/AM was added to cells at a concentration of 5 μM at 30°C for 30 min. Dilution of the cell suspension (5:1) with fresh buffer minimized the concentration of unloaded dye, and time was then allowed for cleavage of internalized fluo-3/AM. Loaded myocytes were excited at 488 nm, with emission collected above 515 nm through a long-pass barrier filter.

To investigate mitochondrial calcium ($[Ca^{2+}]_m$), we used the fluorescent Ca^{2+} probe Rhod-2, a molecule that has a net positive charge allowing its sequestration into mitochondria. This localization was further accentuated through addition of a small excess of sodium borohydride in a methanol solution, which reduced the probe to dihydro Rhod-2 (DHRhod2), favoring preferential compartmentalization in the mitochondrial matrix (Hajnoczky et al., 1995; Mix et al., 1994). Cells were loaded at an approximate concentration of 10 μM DHRhod2 at 30°C for 30 min. Rhod-2 was excited at 514 nm, with emission monitored through a 580-nm (32-nm band pass) barrier filter.

An examination of the intracellular distribution of DHRhod2 was made through comparison with the staining pattern of the mitochondrial-specific probe MitoTracker Green, a molecule that covalently binds to the inner mitochondrial membrane and fluoresces independently of $\Delta\Psi_m$ and $[Ca^{2+}]_m$. For co-localization studies, both fluorophores were excited at 488 nm with emission of MitoTracker Green (522 ± 22 nm) separated from that of DHRhod2 (580 ± 16 nm) through careful selection of emission beam splitters and barrier filters. Signal bleed-through of either probe was determined on cells loaded with only one probe and imaged using identical settings (gain, iris, and black level), concentrations, and incubation times to those used in co-localization studies.

The fluorescent probe JC-1 (5,5′,6,6′-tetrachloro-1,1′,3,3′-tetraethylbenzimidazolcarbocyanine iodine) was used to investigate $\Delta\Psi_m$. JC-1 was excited at 488 nm, the emission split and monitored in dual detectors at 522 nm (35-nm band pass) and 580 nm (32-nm band pass), representing monomer and J-aggregate fluorescence, respectively. The derivation of the ratio of the monomer to aggregate fluorescence provides a measure directly related to $\Delta\Psi_m$ (Simpson and Russell, 1996; Reers et al., 1991, 1995; Smiley et al., 1991; Di Lisa et al., 1995).

Image acquisition and analysis

A suitable image-acquisition mode was determined for each fluorophore being used in a given experiment. Five consecutive 768- × 512-pixel images (1-s scan rate) were averaged (Kalman algorithm) to provide images of DHRhod-2 fluorescence. A similar acquisition mode was used for JC-1 fluorescence, except that dual channels simultaneously monitored both monomer and aggregate fluorescence. Background fluorescence levels (average intensities derived from nonloaded cells at the same gain settings) were subtracted from each component image, and a ratio image was derived through pixel-by-pixel division using a routine written in the BioRad macro programming language (available upon request). Fluorescence intensity histograms were derived for both DHRhod-2 and ratio JC-1 images to determine the average global pixel intensity across the entire cell or from subcellular regions of interest.

Selection criteria for "black hole" areas included that they initially have uptake of DHRhod2 but show significant loss of fluorescence thereafter, and be recognized as an area no more than 4 μm in diameter and 30 gray levels less than the surrounding area. To determine the proportion of the myocyte lacking DHRhod2 fluorescence, we measured the total area of the black holes and expressed it as a fraction of the cell cross-sectional area.

Fluo-3-loaded cells exhibiting spontaneous calcium waves were imaged using line-scan 768- × 512-pixel images (Williams et al., 1992). Orientation of a single raster line along the long axis of the myocyte allowed generation of *X-T* plots, which combined cell length and fluo-3 intensity information at high time resolution. The duration of each total image scan was set to 12 s, which generally allowed for capture of several propagating Ca^{2+} waves. These plots were then used to calculate parameters of the propagating calcium waves, including basal fluorescence intensity, wave frequencies and propagation rates, and the time taken for 50% of the $[Ca^{2+}]_i$ to be removed from the cytosol ($T_{0.5}$) after a Ca^{2+} elevation.

Reagents

Fluo-3/AM, Rhod-2/AM, JC-1, and MitoTracker Green were obtained from Molecular Probes, Eugene, OR. All esterified fluorescent probes were prepared as stock solutions in dimethylsulfoxide (DMSO).

Mitochondrial uncoupler and respiratory chain inhibitors were added to the bathing solution with the concentrations and times of addition as indicated. Carbonyl cyanide *m*-chlorophenylhydrazone (CCCP) and antimycin A were prepared as stock solutions in DMSO. NaCN was prepared as a stock solution in pure water. CCCP, antimycin A, DMSO, cyclosporin A, HEPES, and NaCN were from Sigma-Aldrich (St. Louis, MO)

Statistical analysis

Where appropriate, data are expressed as mean ± SE, where *n* refers to the number of cells studied.

RESULTS

Properties of cytosolic calcium fluxes after addition of mitochondrial inhibitors

Spontaneously contracting cells were examined by a time series of 12-s line-scan images (one line-scan image every 2 min, for up to 30 min). This time period allowed for establishment of control contractile and fluo-3 fluorescence ($[Ca^{2+}]$) profiles for comparison with the responses to subsequent treatment (uncoupling of mitochondria or inhibition of cytochrome *c* oxidase).

Fig. 1 shows a line-scan recording from a single cardiac muscle cell after treatment with 10 mM NaCN, an inhibitor of mitochondrial cytochrome *c* oxidase. Fig. 1 *A* (time 0) illustrates several spontaneous Ca^{2+}-release events (waves) initiated at sites within the cell. The overlaid intensity profile indicates that at a given point within the cell the time course of fluorescence change is remarkably constant, achieving similar peak intensity and declining at a constant rate to a fixed fluorescence level after each transient change.

The addition of NaCN caused a marked progressive change in intracellular fluorescence intensity and in the properties of the propagating Ca^{2+} waves (Fig. 1). In Fig. 1, *B*, *C*, and *D* (6, 12, and 22 min after initiation of treatment), evidence is provided for a progressive reduction of the rate of fluorescence decline (longer decay half-time $T_{0.5}$) in each transient, superimposed on a progressively increasing baseline fluorescence level. Evaluation of an effect on the rate of fluorescence increase in each transient is difficult in the data presented. Although after NaCN treatment the rate of propagation of the waves did not vary markedly, as evidenced by the slope of the fluorescence bands (Fig. 1, *A*–*C*), the initiation of spontaneous Ca^{2+} waves did eventually cease (Fig. 1 *D*).

A summary of the changes in $T_{0.5}$ and basal fluorescence intensity that occurred in individual cells after application of mitochondrial inhibitors (NaCN and antimycin A) and uncoupler (CCCP) is shown in Fig. 2. All additions caused marked increases in $T_{0.5}$, which were evident within 2 min of application of the reagent. Increases in basal fluorescence were generally not evident until later in the time course. Typically, 8–10 min after addition of inhibitor, waves ceased, yet cytosolic fluorescence intensity continued to rise, often culminating in cell hypercontracture.

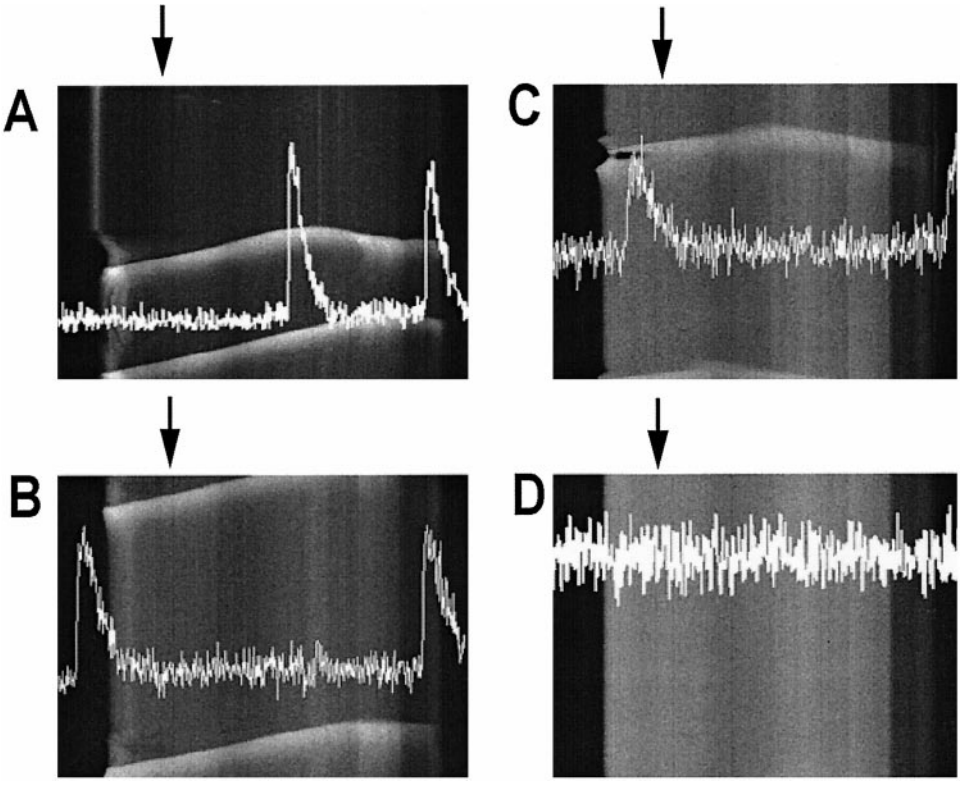

FIGURE 1 A series of line-scan (*X*-*T*) plots from a spontaneously contracting cardiac muscle cell treated with 10 mM NaCN. (*A*) Control, pre-NaCN; (*B*) 6 min after NaCN; (*C*) 12 min after NaCN; (*D*) 22 min after NaCN. Each line-scan image is generated through the repeated scanning over a 12-s period of a raster line orientated along the long axis of the myocyte. Each of the 512 lines of the image requires 23 ms of acquisition time. The high-intensity diagonal bands represent the propagation of a fluo-3 fluorescence wave through the cell. Changes in cell length are seen as the horizontal narrowing of each profile. Overlaid on each profile is a graphical representation illustrating the time course of Ca^{2+} waves through the cell cytosol (*arrow* indicates location of profile).

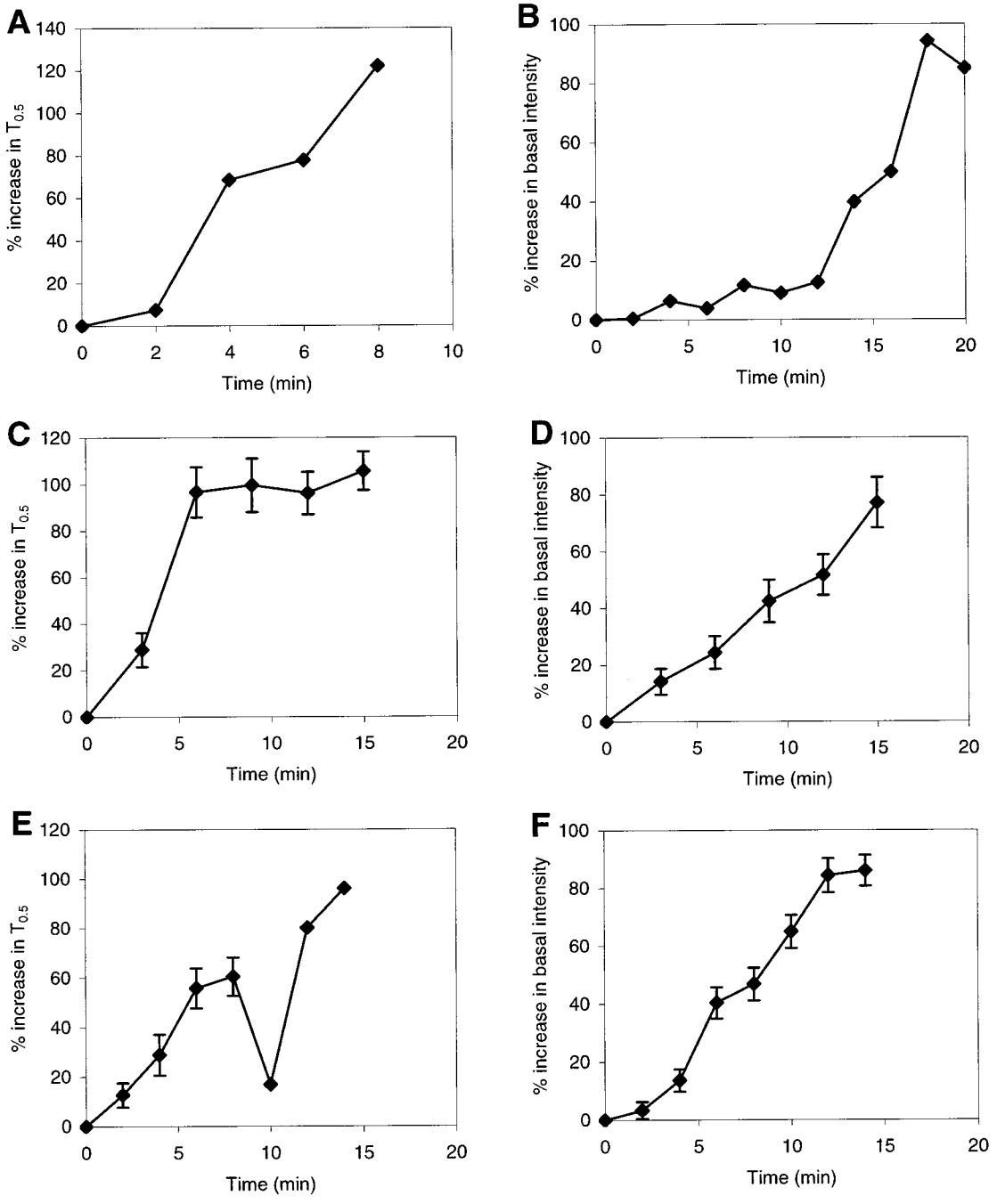

FIGURE 2 Changes in the basal fluorescence intensity and $T_{0.5}$ of Ca^{2+} transients after addition of uncouplers or inhibitors of mitochondrial respiration. Effects of addition of 10 mM NaCN (*A*, *B*; $n = 9$ cells), 0.5 nM antimycin A (*C*, *D*; $n = 7$), and 40 nM CCCP (*E*, *F*; $n = 4$) on $T_{0.5}$ (*A*, *C*, and *E*) and basal fluorescence intensity (*B*, *D*, *E*) are depicted. All graphs express data as the percentage increase from the pretreatment values. Data are expressed as mean ± SEM.

An interesting and fundamentally important observation was the increasing number of fluorescence hotspots (Fig. 3), now commonly known as focal areas of Ca^{2+} release (Williams, 1993), or Ca^{2+} sparks (Cheng et al., 1996). The Ca^{2+} sparks occurred soon after addition of NaCN and continued until the cessation of Ca^{2+} waves. Increased numbers of Ca^{2+} sparks occurred predominantly after a single propagating Ca^{2+} wave but were also evident between individual waves.

Alteration of mitochondrial membrane potential

It was anticipated that the ability of these added reagents to cause significant changes in the dynamics of intracellular Ca^{2+} fluxes was due to their ability to disrupt or alter mitochondrial membrane potential ($\Delta\Psi_m$). This possibility was investigated in cells loaded with JC-1, a ratiometric indicator of $\Delta\Psi_m$. Dual-channel emission images of JC-1-loaded, quiescent cardiac cells illustrated the heterogeneous

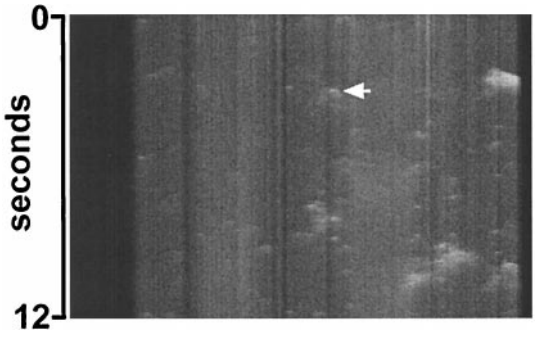

FIGURE 3 Line-scan (*X-T*) plot of Ca^{2+} sparks in a cell treated with NaCN (10 mM). Shown is a 12-s line-scan plot of a fluo-3-loaded cardiac myocyte. The localized high-intensity regions throughout the profile represent spontaneous Ca^{2+} sparks (*arrow*). The sparks appear as small vertical lines in the line-scan due to the time taken (12 s) to generate the image.

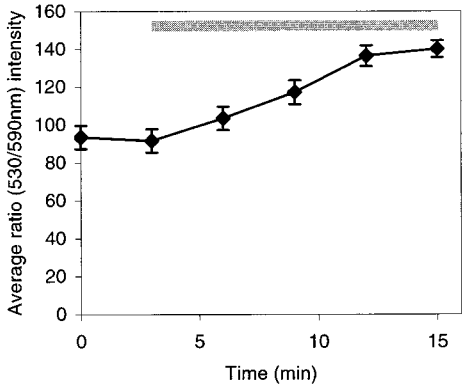

FIGURE 5 Ratio of JC-1 fluorescence changes upon treatment of cardiac cells with 0.5 nM antimycin A. Shown is the change in the average ratio (scaled by a factor of 100) of JC-1 fluorescence (intensity units) after addition of antimycin A (0.5 nM). The data shown are the means ± SEM for seven cardiac cells. The bar indicates treatment duration.

nature of $\Delta\Psi_m$. Although the monomer fluorescence intensity was relatively homogeneous throughout an individual cell, J-aggregate fluorescence was heterogeneous with a higher intensity observed within 5–10-μm of the cell edge (sarcolemma; Fig. 4). Quiescent cells exhibited a JC-1 fluorescence ratio that was constant over a 60-min period. Addition of either a mitochondrial electron transport chain inhibitor (NaCN or antimycin A) or a protonophore (CCCP) caused depression of $\Delta\Psi_m$. This depression of $\Delta\Psi_m$ was also apparent in spontaneously contracting cells as illustrated in Fig. 5 for a cell treated with antimycin A ($n = 7$). Of particular interest was the time course of the change of $\Delta\Psi_m$ after addition of reagent, with the decrease commencing almost immediately after addition of antimycin A (Fig. 5) and the potential then remaining constant after 12 min. Fluorescence changes with similar time course were evident after CCCP (40 nM) and NaCN (10 mM) addition (data not shown). Although the overall cellular ratio fluorescence decreased, discrete alterations in the aggregate fluorescence were also apparent in the images. These alterations consisted of localized increases or decreases in the aggregate fluorescence, suggesting localized elevations or depressions of $\Delta\Psi_m$, respectively.

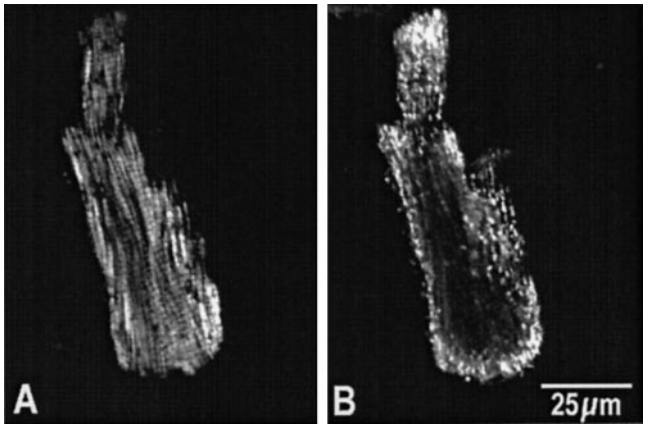

FIGURE 4 Dual-channel recording of the distribution of JC-1 fluorescence in a cardiac myocyte. JC-1 was excited with the 488-nm band of an Ar ion laser. (*A*) Monomer fluorescence image (522 ± 35-nm band pass). (*B*) J-aggregate fluorescence image (580 ± 32-nm band pass). Note that the distribution of JC-1 potential-insensitive monomer is relatively homogeneous throughout the cell (*A*) compared with the regional differences in fluorescence of potential-sensitive J-aggregate (*B*).

Mitochondrial calcium changes

To determine whether the altered Ca^{2+} fluxes resulting from changes in $\Delta\Psi_m$ were dependent on mitochondrial sources of Ca^{2+}, the Ca^{2+} indicator DHRhod2 was used to selectively monitor this Ca^{2+} pool. Quiescent cells loaded with DHRhod2 exhibited a regular, banded fluorescence pattern, typical of the cardiac mitochondrial distribution (Fig. 6). Mitochondrial localization of fluorescence was confirmed through the co-loading of DHRhod2 with the mitochondrial-specific probe MitoTracker Green. In addition, treatment of DHRhod2-loaded cells with 0.2 mM $MnCl_2$ for 30 min at 37°C, a manipulation known to quench cytosolic fluorescence, caused no significant change in the fluorescence pattern (data not shown).

Interestingly, many spontaneously contracting cells demonstrated discrete black holes in the otherwise regular, banded DHRhod-2 fluorescence pattern. Although these may have simply represented irregularities in the fluorescence staining of small groups of mitochondria, addition of 10 mM NaCN to cells caused the number of these black holes to increase progressively over a 50-min period, thereby eliminating this possibility (data not shown). As NaCN indirectly causes depression of $\Delta\Psi_m$, these black holes are likely to represent individual or small groups of mitochondria that have lost accumulated DHRhod-2 and/or Ca^{2+}.

This proposition was investigated more closely as follows. Cells were co-loaded with DHRhod2 and MitoTracker Green and then treated with 10 mM NaCN. Images were taken at 2-min intervals over a 1-h period, allowing the construction of a time-lapse image series that is shown in

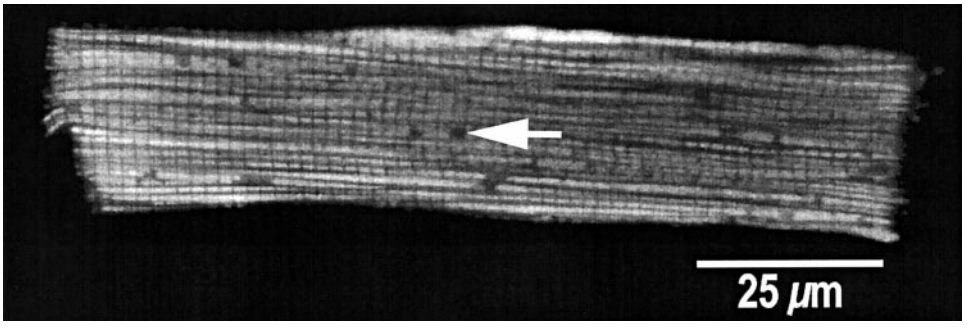

FIGURE 6 Typical fluorescence pattern of a di-hydro-rhod-2-loaded cardiac cell. The compartmentalized, banded fluorescence pattern, typical of mitochondrial distribution in cardiac myocytes, is evident. The arrow indicates a discrete region of extremely low fluorescence intensity, a black hole, indicating potential loss of mitochondrial Ca^{2+} or rhod-2. Excitation, 488 nm; emission, 580 ± 32 nm.

Fig. 7. The initially low number of these discrete black holes in the DHRhod2 fluorescence pattern did not appear to increase markedly until 30 min after exposure to NaCN. The total cell fluorescence then rapidly declined until 50 min after addition of reagent, at which point cells began to hypercontract. Each appearance of a black hole in the DHRhod2 fluorescence occurred simultaneously with a localized increase in the MitoTracker Green fluorescence (Fig. 8). This confirms the mitochondrial origin of black holes. Note in Fig. 7 that there are discontinuities in the image (thin arrowheads), which are not considered black holes as they are evident before NaCN addition and the origin of which is as yet undetermined. These observations are not consistent with the possibility of fluorescence resonance energy transfer (FRET) between fluorophores as both were co-excited in these experiments, and the observations were identical when the fluorophores were used individually. Although this localized fluorescence increase dissipated in the ensuing 6-min period, the average intracellular fluorescence of MitoTracker Green gradually increased throughout the image acquisition period.

To examine the possibility that the black holes result from opening of the MPT pore, the effect of cyclosporin A on their formation was studied. Addition of cyclosporin A (1 μM) 30 min before addition of NaCN (10 mM) almost completely abolished the emergence of black holes (Fig. 9). These observations indicated that the loss of fluorescence leading to the appearance of black holes was due to induction of opening of the MPT pores.

DISCUSSION

The results presented in this study demonstrate that the propagation of spontaneous Ca^{2+} waves in cardiac myocytes is influenced by mitochondrial function. Uncoupling of mitochondria or inhibition of cytochrome *c* oxidase caused depression of $\Delta\Psi_m$, rapidly leading to a reduction in the rate of removal of Ca^{2+} from the cytosol after a Ca^{2+} transient. Additionally, examinations of mitochondrial Ca^{2+} content, particularly in spontaneously contracting cardiac myocytes, revealed small groups of mitochondria devoid of Ca^{2+}. To our

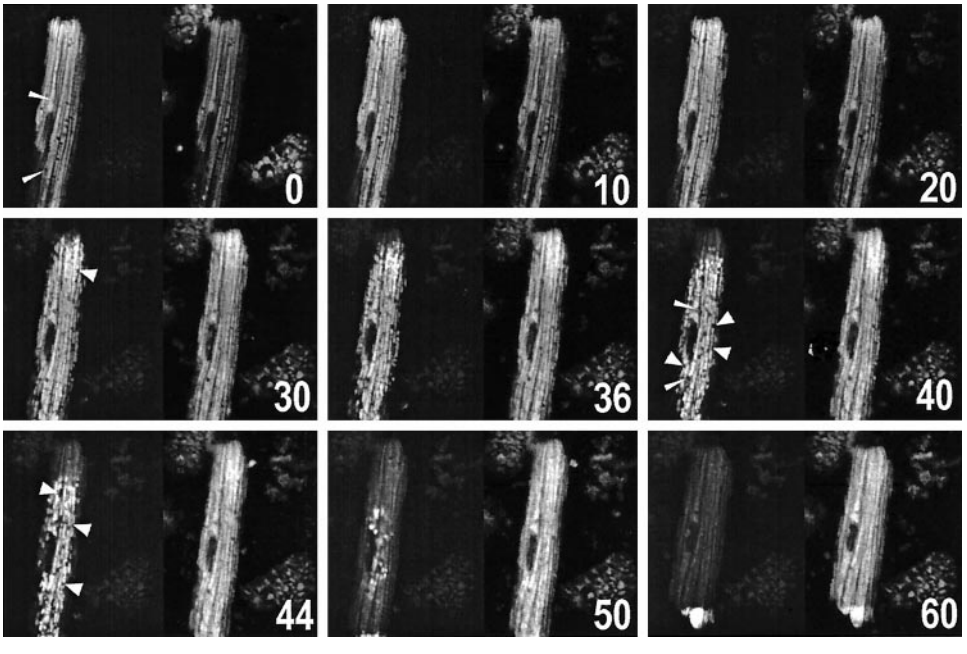

FIGURE 7 Loss of mitochondrial Ca^{2+} in NaCN-inhibited mitochondria. The time series of nine frames was collected over a 60-min period where each frame represents a dual-channel recording of DHRhod2 (*left*) and MitoTracker Green (*right*). Numbers in the bottom right-hand corner indicate time (min) after addition of 10 mM NaCN to the bathing solution. Thin arrowheads indicate invariant discontinuities not considered black holes at 0 and 40 min. Thick arrowheads point to different individual black holes at various times.

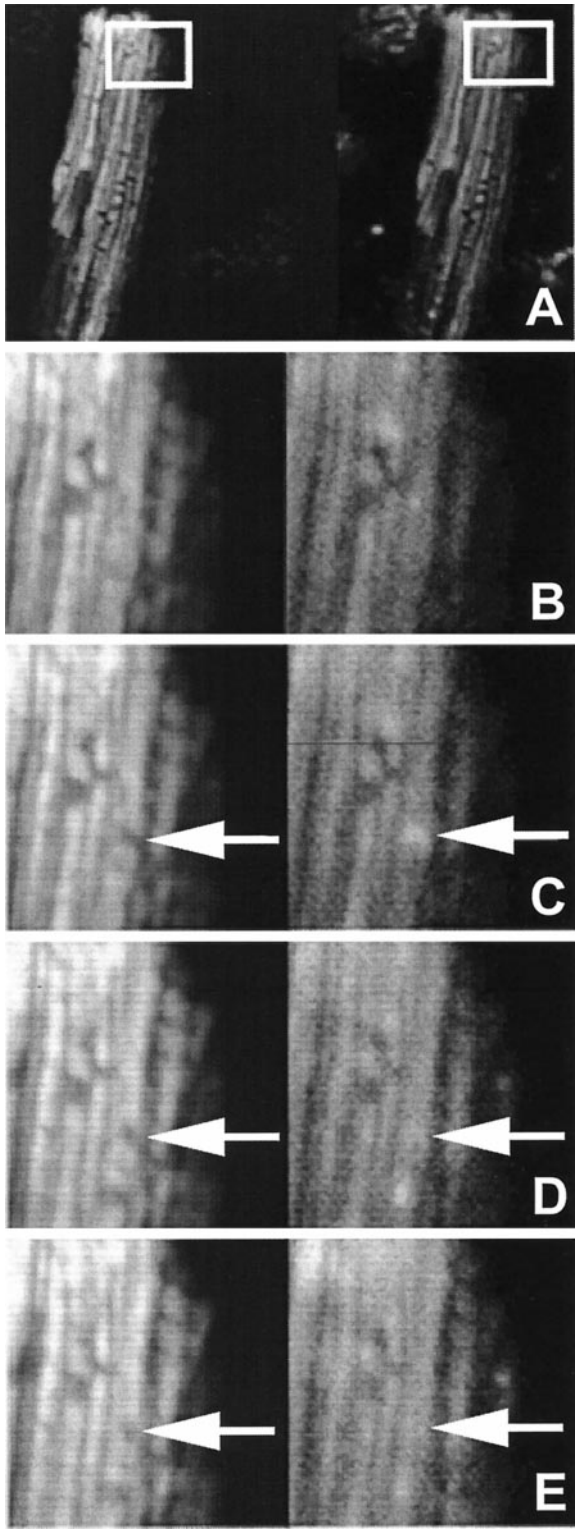

FIGURE 8 Localized fluorescence changes in NaCN-uncoupled mitochondria. (*A*) Dual-channel recording of DHRhod2 (*left*) and MitoTracker Green (*right*). Areas in white boxes indicate the regions magnified in *B–E*. Images were taken at the following times subsequent to addition of NaCN: 6 min (*B*), 8 min (*C*), 10 min (*D*), and 12 min (*E*). Loss of mitochondrial Ca^{2+} (appearance of a black hole) occurs simultaneously with localized increase in the MitoTracker Green fluorescence (*arrow*). This high-intensity fluorescence dissipates over the ensuing 6-min period.

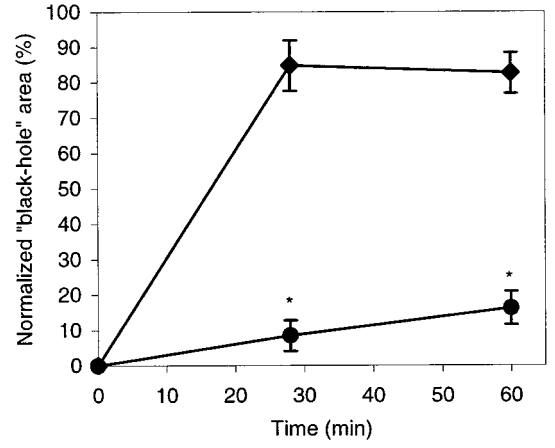

FIGURE 9 The effect of cyclosporin A on black hole formation in cardiomyocytes after addition of 10 mM NaCN. To determine the proportion of the cell containing black holes, we measured the area of the cell lacking DHRhod2 fluorescence and expressed this as a proportion of the total cell area. The figure expresses the percentage change in the black hole area normalized at each time point with respect to the fluorescence in that particular area at 0 min. Criteria for black hole selection included that they be no more than 4 μm in diameter and approximately 30 gray levels less than the surrounding area. Data are expressed as mean ± SEM. Significant differences between cyclosporin-A-treated (●) and untreated (♦) myocytes were determined using a Student Newman-Keuls post hoc analysis ($*p < 0.01$; $n = 5$ for both treatment groups).

knowledge, images such as these illustrating the loss of mitochondrial Ca^{2+} have not been previously reported.

Mitochondrial involvement in Ca^{2+} wave propagation

A role for mitochondria in the regulation of cytosolic Ca^{2+} has been long thought to be important only in pathophysiological conditions. This view has been supported by studies of permeabilized cardiac myocytes that demonstrated that significant mitochondrial calcium uptake did not occur until the cytoplasmic calcium exceeded 1 μM (Fry et al., 1984). These studies provided evidence for a role of mitochondrial Ca^{2+} transport systems for regulating mitochondrial $[Ca^{2+}]$ but not support for a significant involvement in the regulation of cytosolic $[Ca^{2+}]$. However, evidence for a role of mitochondrial calcium uptake under normal physiological conditions, particularly after spontaneous calcium transients, has been gathering in recent years. Jouaville et al. (1995), investigating inositol-1,4,5-trisphosphate-induced Ca^{2+} release in *Xenopus* oocytes, energized mitochondria with pyruvate/malate and observed increased Ca^{2+} wave amplitude and velocity. These effects were blocked by rotenone (an inhibitor of mitochondrial complex I) and antimycin A. Drummond and Fay (1996) investigated calcium release in electrically stimulated smooth muscle cells and demonstrated that NaCN or FCCP significantly increased the half-time for Ca^{2+} removal ($T_{0.5}$) without altering resting cytosolic calcium concentration.

Our results showed increases in $T_{0.5}$ after addition of NaCN, antimycin A, or CCCP and at face value are in agreement with both studies. However, after prolonged exposure, the spontaneous Ca^{2+} waves eventually ceased and basal cytosolic calcium gradually increased. Although this may be due in part to the release of mitochondrial calcium, it is unlikely that such an effect alone could fully explain the observation we have made. The treatments are also likely to have modified the function of intracellular compartments that contribute to establishing basal $[Ca^{2+}]_i$, as well as affecting the activity or concentration of pumps and Ca^{2+} buffers that may contribute to Ca^{2+} homeostasis. Additional work will identify the relative contribution of these possibilities.

Mitochondrial membrane potential alterations in spontaneously contracting cardiac myocytes

Uptake of Ca^{2+} by mitochondria is dependent on the potential difference across the mitochondrial membranes. By reducing $\Delta\Psi_m$, the activity of the Ca^{2+} uniporter influx is reduced. Therefore CCCP, NaCN, and antimycin A would indirectly inhibit mitochondrial Ca^{2+} uptake through the depression of $\Delta\Psi_m$. This depression was demonstrated using JC-1, a lipophilic cation, which distributes across the mitochondrial membrane in a fashion accurately described by the Nernst equation. JC-1 normally exists in its monomeric form. However, upon accumulation in the mitochondrial matrix, JC-1 forms J-aggregates, with different emission spectral characteristics, in proportion to mitochondrial membrane potential. The complete depression of $\Delta\Psi_m$ by treatment with respiratory inhibitors or uncouplers took approximately 15 min as judged by the time required to establish a new steady-state level, a time that is in agreement with values quoted in other studies on rat cardiac myocytes (Di Lisa et al., 1995). In the study of Di Lisa and colleagues, a decrease in $\Delta\Psi_m$ was demonstrated at the onset of anoxia, whereas contractile activity was retained. The $\Delta\Psi_m$ then collapsed at the onset of rigor. In the present study, the time course of changes in Ca^{2+} wave activity indicates that whereas $\Delta\Psi_m$ was decreasing, Ca^{2+} waves and contractile activity were still present but in most cells had ceased once the $\Delta\Psi_m$ reached a constant depressed level. In the meantime, $[Ca^{2+}]_i$ continued to gradually rise. Control studies of untreated, spontaneously contractile cells indicated that many myocytes continue activity for greater than 30 min, and it is clear that the cessation of spontaneous calcium transients is due to the decrease in $\Delta\Psi_m$ induced by respiratory inhibitors and uncouplers.

Mitochondrial calcium changes after uncoupling of the respiratory chain

Through depression of $\Delta\Psi_m$ and inhibition of Ca^{2+} uptake, resting $[Ca^{2+}]_i$ increases. Clearly, this could be due to the involvement of several processes, including an absence of mitochondrial Ca^{2+} regulatory mechanisms, inhibition of SR and sarcolemmal Ca^{2+}-ATPases, or the release of mitochondrial calcium. There is evidence to suggest that after depression of $\Delta\Psi_m$, the ruthenium red-sensitive mitochondrial Ca^{2+} uniporter may reverse direction, allowing efflux of Ca^{2+} into the cytosol (Nicholls and Åckerman, 1982). Additional efflux of mitochondrial Ca^{2+} can occur through induction of the mitochondrial permeability transition (MPT). The molecular structure and mechanisms of inhibition and activation of this MPT pore have been the subject of numerous investigations, summarized in many reviews and symposium proceedings (Zoratti and Szabo, 1995; Bernardi, 1996). From the collective data it is generally agreed that the MPT pore is a large, proteinaceous, Ca^{2+}-activated, proton- and ADP-inhibited, voltage-dependent pore, spanning the inner and outer mitochondrial membranes, allowing the passage of ions and substrates less than 1.5 kDa. The MPT has been implicated in cell death processes, particularly in cellular ischaemia- and reperfusion-induced injury (Crompton and Costi, 1990; Griffiths and Halestrap, 1995), and in the induction of apoptosis (Mignotte and Vayssierre, 1998). Characteristically, opening of the MPT pore is inhibited by cyclosporin A (Zoratti and Szabo, 1995; Bernardi, 1996).

When quiescent cardiac cells were loaded with DHRhod-2, the normal, banded fluorescence pattern was observed. However, there were irregular black holes in the regular compartmentalized pattern. Such black holes could represent single or groups of mitochondria that have expelled Ca^{2+} from the matrix, have lost accumulated Rhod-2 due to depressed $\Delta\Psi_m$, or may never have accumulated DHRhod2. After addition of NaCN to these cells, we observed a gradual decrease in the total cell Rhod-2 fluorescence. These observations can be explained if the treatments undertaken caused an induction of the MPT, providing a pathway for the loss of constituents such as Ca^{2+} and DHRhod2 from mitochondria. This possibility is strengthened by the finding that cyclosporin A, an inhibitor of MPT induction, largely prevented the loss of these mitochondrial solutes.

Time course of changes after uncoupling of the mitochondrial respiratory chain

Numerous observations with a variety of fluorescent probes examining cellular and mitochondrial function have allowed us to develop a model describing the time course of these events (Fig. 10). The illustration describes two phases after uncoupling of the mitochondrial respiratory chain. These phases are not distinct, but overlap, allowing a discussion of the concurrent observations made.

Immediately after addition of, for example, NaCN (first phase), DHRhod-2 fluorescence intensity fluctuated throughout the cell, indicating calcium fluctuations within mitochondria. At this time, average $\Delta\Psi_m$ across the cell was gradually depressed, thereby reducing the activity of the Ca^{2+} uniporter. Alternatively, the changes in $[Ca^{2+}]_m$ and

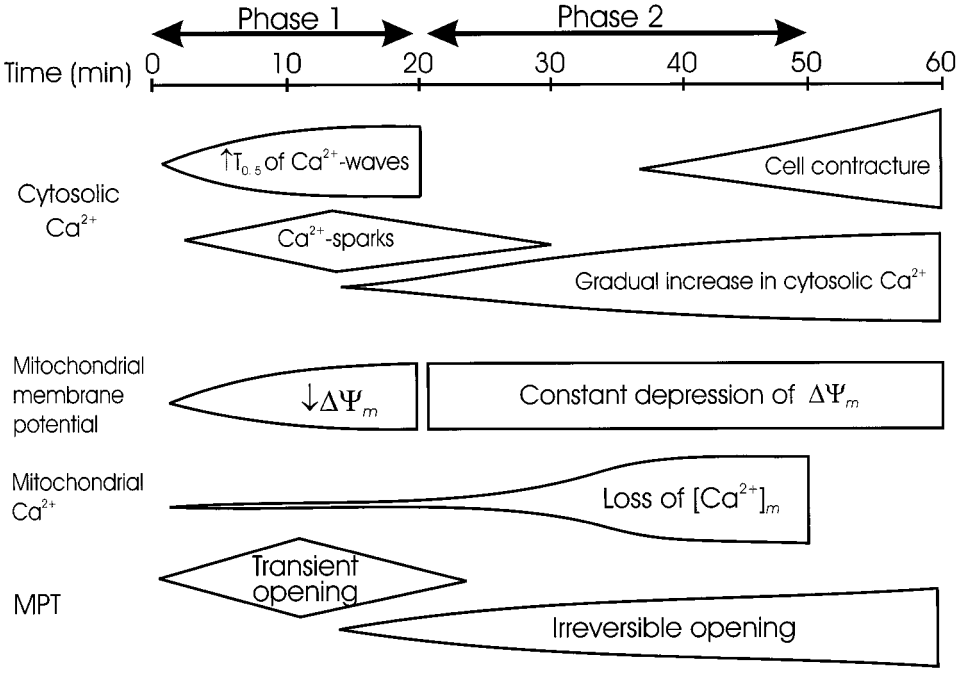

FIGURE 10 Schematic representation of time course of changes after disruption of mitochondrial function in cardiac cells. This diagram represents the temporal relationship between the observed changes in cytosolic Ca^{2+} (fluo-3), mitochondrial membrane potential (JC-1), and mitochondrial Ca^{2+} (DHRhod-2) over a 60-min period after inhibitors and uncouplers of the mitochondrial respiratory chain. The inferred changes in the open probability of the mitochondrial permeability transition pore are also displayed. The magnitude of the change in each parameter is reflected in the breadth of the profile at any time point. See text for a description of the phases.

$\Delta\Psi_m$ may indicate the transient opening of the MPT in a low-conductance mode. Previous studies by Ichas and colleagues (1994, 1997) have demonstrated oscillating open and closed states of the pore in a low-conductance mode, supporting a mechanism termed the mitochondrial calcium-induced calcium release. This experimental evidence illustrated a process whereby uptake of calcium into mitochondria reached a threshold concentration, activating the MPT and releasing calcium into the cytosol. This cyclical process enabled mitochondria to propagate a calcium transient between adjacent mitochondria and therefore throughout the cell.

The end of phase one involved a minor increase in the number of black holes with no observed change in the average cell DHRhod-2 fluorescence intensity. This may indicate that some mitochondria possess MPT pores that were operating in a high-conductance state. This state is irreversible, allowing the rapid loss of mitochondrial calcium and other low molecular weight metabolites (Hunter and Haworth, 1979a,b; Vercesi et al., 1988). A major decrease in the overall cellular fluorescence does not occur until phase two, at which point there is a rapid decline in the compartmentalized fluorescence of Rhod-2. The fluorescence decline begins in mitochondria close to the cell sarcolemma and progress inward to the center of the cell. This may indicate rapid loss of calcium though the high-conductance MPT pore. However, the decline in fluorescence may either be due to loss of charged DHRhod2 due to reduction of the mitochondrial membrane potential or through the open pores. The decline in the DHRhod2 fluorescence begins close to the cell membrane and correlates well with the loading patterns of JC-1. Higher J-aggregate fluorescence (and therefore higher $\Delta\Psi_m$) was also observed in this region, perhaps indicating that these mitochondria with higher resting $\Delta\Psi_m$ are the first to lose accumulated calcium. The underlying mechanism is not yet clear but may be related to the kinetics of diffusion of NaCN into the myocyte preparations.

In the first phase after addition of NaCN, antimycin A, or CCCP, an increased number of spontaneous nonpropagating Ca^{2+}-release events, or Ca^{2+} sparks, was also evident. The events underlying Ca^{2+} sparks represent the release of Ca^{2+} from one or a group of SR ryanodine receptors (Cannell et al., 1994; Cannell et al., 1995). Under normal conditions, Ca^{2+} sparks underlie excitation-contraction coupling, whereby opening of L-type Ca^{2+} channels causes a small influx of Ca^{2+}, which subsequently acts on ryanodine receptors to cause Ca^{2+} release that, when synchronized, leads to contraction. Although observation of Ca^{2+} sparks in spontaneously active cardiac myocytes has been made in several previous studies, the present data suggest that release of mitochondrial Ca^{2+} through the transient MPT activity may provide a $[Ca^{2+}]_i$ change of sufficient local magnitude and rate of change ($\Delta[Ca^{2+}]/\Delta t$) to activate or contribute to Ca^{2+} sparks. Electron microscopic studies have demonstrated that mitochondria occupy a significant proportion of the total cell volume (~30%) and that they are in close proximity to adjacent SR. Although such an arrangement would allow the diffusion of released mitochondrial Ca^{2+} to reach SR ryanodine receptors (Bassani et al., 1993), whether the increased Ca^{2+} would be sufficient to induce CICR before sequestration by SR Ca^{2+}-ATPases is unknown. Other studies that have alluded to mitochondrial involvement (Cannell et al., 1994; Cheng et al., 1996) have focused on passive effects such as mitochondria providing a physical obstruction to calcium diffusion, thereby affecting patterns of Ca^{2+} release. This is one of the first studies to have

described a direct active contribution of mitochondria to initiation or propagation of Ca^{2+} release in cardiac muscle.

CONCLUSION

We have been able to image various functional properties of mitochondria in isolated cardiomyocytes. In isolation, these techniques have enabled the development of a working model as a foundation for examining the time course of events surrounding spontaneous contractile activity and the underlying calcium dynamics (intracellular and mitochondrial), believed ultimately to lead to ventricular arrhythmia and cell death. However, additional experimental evidence is required to examine fully the hypothesis that the transient opening of the MPT, and its release of Ca^{2+}, are involved in the development of spontaneous contractions and subsequent arrhythmia.

REFERENCES

Bassani, J. W., R. A. Bassani, and D. M. Bers. 1993. Ca^{2+} cycling between sarcoplasmic reticulum and mitochondria in rabbit cardiac myocytes. *J. Physiol. (Lond.).* 460:603–621.

Bernardi, P. 1996. The permeability transition pore: control points of a cyclosporin A-sensitive mitochondrial channel involved in cell death. *Biochim. Biophys. Acta.* 1275:5–9.

Bers, D. M. 1991. Excitation-Contraction Coupling and Cardiac Contractile Force. Kluwer Academic Publishers, Dordrecht, The Netherlands.

Biscoe, T. J., M. R. Duchen, D. A. Eisner, S. C. O'Neill, and M. Valdeolmillos. 1989. Measurement of intracellular Ca^{2+} in dissociated type I cells of rabbit carotid body. *J. Physiol. (Lond.).* 416:421–434.

Cannell, M. B., H. Cheng, and W. J. Lederer. 1994. Spatial nonuniformities in $[Ca^{2+}]_i$ during excitation-contraction coupling in cardiac myocytes. *Biophys. J.* 67:1942–1956.

Cannell, M. B., H. Cheng, and W. J. Lederer. 1995. The control of calcium release in heart muscle. *Science.* 268:1045–1049.

Cheng, H., M. R. Lederer, R-P. Xiao, A. M. Gomez, Y-Y. Zhou, B. Ziman, H. Spurgeon, E. G. Lakatta, and W. J. Lederer. 1996. Excitation-contraction coupling in heart: new insights from Ca^{2+} sparks. *Cell Calcium.* 20:128–140.

Crompton, M., and A. Costi. 1990. A heart mitochondrial Ca^{2+}-dependent pore of possible relevance to re-perfusion-induced injury: evidence that ADP facilitates pore interconversion between the closed and open states. *Biochem. J.* 266:33–39.

Di Lisa, F., P. S. Blank, R. Colonna, G. Gambassi, H. S. Silverman, M. D. Stern, and R. G. Hansford. 1995. Mitochondrial membrane potential in single living adult rat cardiac myocytes exposed to anoxia or metabolic inhibition. *J. Physiol. (Lond.).* 486:1–13.

Drummond, R. M., and F. S. Fay. 1996. Mitochondria contribute to Ca^{2+} removal in smooth muscle cells. *Pflugers Arch.* 431:473–482.

Fay, F. S., D. A. Williams, G. Kargacin, R. W. Tucker, and M. Scanlon. 1988. Role of local $[Ca^{2+}]$ in the control of cell function. *Adv. Exp. Med. Biol.* 232:213–219.

Fry, C. H., T. Powell, V. W. Twist, and J. P. T. Ward. 1984. Net calcium exchange in adult rat ventricular myocytes: an assessment of mitochondrial calcium accumulating capacity. *Proc. R. Soc. (Lond.)* 223:223–238.

Griffiths, E. J., and A. P. Halestrap. 1995. Mitochondrial non-specific pores remain closed during cardiac ischaemia, but open upon reperfusion. *Biochem. J.* 307:93–98.

Gunter, T. E., and D. R. Pfeiffer. 1990. Mechanisms by which mitochondria transport calcium. *Am. J. Physiol.* 258:C755–C786.

Gunter, K. K., M. J. Zuscik, T. E. Gunter. 1991. The Na^+-independent Ca^{2+} efflux mechanism of liver mitochondria is not a passive $Ca^{2+}/2H^+$ exchanger. *J. Biol. Chem.* 266:21640–21648.

Hajnoczky, G., L. D. Robb-Gaspers, M. B. Seitz, and A. P. Thomas. 1995. Decoding of cytosolic calcium oscillations in the mitochondria. *Cell.* 82:415–424.

Haworth, R. A., and D. R. Hunter. 1979. The Ca^{2+}-induced membrane transition in mitochondria. II. Nature of the Ca^{2+} trigger site. *Arch. Biochem. Biophys.* 195:460–467.

Hunter, D. R., and R. A. Haworth. 1979a. The Ca^{2+}-induced membrane transition in mitochondria. I. The protective mechanisms. *Arch. Biochem. Biophys.* 195:453–459.

Hunter, D. R., and R. A. Haworth. 1979b. The Ca^{2+}-induced membrane transition in mitochondria. III. Transitional Ca^{2+} release. *Arch. Biochem. Biophys.* 195:468–477.

Ichas, F., L. S. Jouaville, and J. P. Mazat. 1997. Mitochondria are excitable organelles capable of generating and conveying electrical and calcium signals. *Cell.* 89:1145–1153.

Ichas, F., L. S. Jouaville, S. S. Sidash, J. P. Mazat, and E. L. Holmuhamedov. 1994. Mitochondrial calcium spiking: a transduction mechanism based on calcium-induced permeability transition involved in cell calcium signalling. *FEBS Lett.* 348:211–215.

Ishide, N., T. Urayama, K. Inoue, T. Komaru, and T. Takishima. 1990. Propagation and collision characteristics of calcium waves in rat myocytes. *Am. J. Physiol.* 259:H940–H950.

Jouaville, L. S., F. Ichas, E. L. Holmuhamedov, P. Camacho, and J. D. Lechleiter. 1995. Synchronization of calcium waves by mitochondrial substrates in *Xenopus laevis* oocytes. *Nature.* 377:438–441.

Lopez, J. R., A. Jovanovic, and A. Terzic. 1995. Spontaneous calcium waves without contraction in cardiac myocytes. *Biochem. Biophys. Res. Commun.* 214:781–787.

Marchetti, P., M. Castedo, S. A. Susin, N. Zamzami, T. Hirsch, A. Macho, A. Haeffner, F. Hirsch, M. Geuskens, and G. Kroemer. 1996. Mitochondrial permeability transition is a central coordinating event of apoptosis. *J. Exp. Med.* 184:1–6.

McCormack, J. G., A. P. Halestrap, and R. M. Denton. 1990. Role of calcium ions in regulation of mammalian intramitochondrial metabolism. *Physiol. Rev.* 70:391–425.

Mignotte, B., and J.-L. Vayssiere. 1998. Mitochondria and apoptosis. *Eur. J. Biochem*. 252:1–15.

Mix T. C. H., R. M. Drummond, R. A. Tuft, and F. S. Fay. 1994. Mitochondria in smooth muscle sequester Ca^{2+} following stimulation of cell contraction. *Biophys. J.* 66:A97.

Miyata, H., H. S. Silverman, S. J. Sollott, E. G. Lakatta, M. D. Stern, and R. G. Hansford. 1991. Measurement of mitochondrial free Ca^{2+} concentration in living single rat cardiac myocytes. *Am. J. Physiol.* 261: H1123–H1134.

Nicholls, D., and K. Åckerman. 1982. Mitochondrial calcium transport. *Biochim. Biophys. Acta.* 683:57–88.

Puskin, J. S., Gunter, T. E., Gunter, K. K., and P. R. Russell. 1976. Evidence for more than one Ca^{2+} transport mechanism in mitochondria. *Biochemistry.* 15:3834–3842.

Reers, M., S. T. Smiley, C. Mottola Hartshorn, A. Chen, M. Lin, and L. B. Chen. 1995. Mitochondrial membrane potential monitored by JC-1 dye. *Methods Enzymol.* 260:406–417.

Reers, M., T. W. Smith, and L. B. Chen. 1991. J-aggregate formation of a carbocyanine as a quantitative fluorescent indicator of membrane potential. *Biochemistry.* 30:4480–4486.

Simpson, P. B., and J. T. Russell. 1996. Mitochondria support inositol 1,4,5-trisphosphate-mediated Ca^{2+} waves in cultured oligodendrocytes. *J. Biol. Chem.* 271:33493–33501.

Smiley, S. T., M. Reers, C. Mottola Hartshorn, M. Lin, A. Chen, T. W. Smith, G. D. Jr. Steele, and L. B. Chen. 1991. Intracellular heterogeneity in mitochondrial membrane potentials revealed by a J-aggregate-forming lipophilic cation JC-1. *Proc. Natl. Acad. Sci. U.S.A.* 88: 3671–3675.

Takamatsu, T., and W. G. Wier. 1990. Calcium waves in mammalian heart: quantification of origin, magnitude, waveform, and velocity. *FASEB J.* 4:1519–1525.

Trollinger, D. R., W. E. Cascio, and J. J. Lemasters. 1997. Selective loading of Rhod 2 into mitochondria shows mitochondrial Ca^{2+} transients during the contractile cycle in adult rabbit cardiac myocytes. *Biochem. Biophys. Res. Commun.* 236:738–742.

Vercesi, A. E., V. L. Ferraz, D. V. Macedo, and G. Fiskum. 1988. Ca^{2+}-dependent $NAD(P)^{+}$-induced alterations of rat liver and hepatoma mitochondrial membrane permeability. *Biochem. Biophys. Res. Commun.* 154:934–941.

Williams, D. A. 1990. Quantitative intracellular calcium imaging with laser-scanning confocal microscopy. *Cell Calcium.* 11:589–597.

Williams, D. A. 1993. Mechanisms of calcium release and propagation in cardiac cells. Do studies with confocal microscopy add to our understanding? *Cell Calcium.* 14:713–724.

Williams, D. A., L. M. Delbridge, S. H. Cody, P. J. Harris, and T. O. Morgan. 1992. Spontaneous and propagated calcium release in isolated cardiac myocytes viewed by confocal microscopy. *Am. J. Physiol.* 262:C731–C742.

Zoratti, M., and I. Szabo. 1995. The mitochondrial permeability transition. *Biochim. Biophys. Acta.* 1241:139–176.